Homoclinic Crossings and Pattern Selection

Hie Tae Moon
Physics Department, Korea Institute of Technology, Daeduk Science-town 305-701, Korea
(Received 11 September 1989)

The correlations between a homoclinic orbit (HMO) and coherent patterns in the nonlinear Schrödinger model are discussed. In a Hamiltonian situation, two independent patterns are revealed to exist: One corresponds to a motion within an HMO, and the other, outside of an HMO. The study further illustrates, when the Hamiltonian constraint is released, the significance of an HMO on the pattern dynamics by presenting the irregular HMO crossings and the resulting chaotic selections between the patterns.

PACS numbers: 47.10.+g, 05.45.+b, 47.20.Ky

When fluctuations or very small perturbations force an existing continuous system into a nonequilibrium situation where instability is possible, the entire system may reorganize itself in such a way as to build patterns of order.[1] The Bénard cell is a striking example. In recent years, the study of coherent patterns in a continuous medium has been a topical research area.[2,3] In this Letter, we discuss the significant role of the presence of a homoclinic orbit (HMO) on the pattern dynamics in a nonlinear dispersive medium.

The model is a one-dimensional medium which is governed by the following nonlinear Schrödinger equation (NLS):

$$i\psi_t+\psi_{xx}+|\psi|^2\psi=0. \tag{1}$$

The NLS is one of the fundamental equations encountered in the modern theory of nonlinear waves. With the form shown in (1), the NLS is the Hamiltonian and possesses infinitely many constants of motion. For initial conditions decaying sufficiently rapidly with large $|x|$, the NLS is integrable by the inverse scattering transform and admits, asymptotically, a finite number of stable solitons.[4] The NLS is also well known to admit the uniform-wave-train solution (also known as the Stokes solution)

$$\psi_e(t)=e^{it}, \tag{2}$$

which is linearly unstable to infinitesimal sideband modulations of the form $a_1\exp(iqx+\Omega t)+a_2\exp(-iqx+\Omega^* t)$. Benjamin and Feir[5] gave the linear growth rate as a function of an unstable wave number as

$$\Omega(q)=(-q^4+2q^2)^{1/2},\quad 0<q<\sqrt{2}. \tag{3}$$

As shown in (3), the maximum instability takes place when $q=q_{\max}=1$. This instability has been referred to as the Benjamin-Feir instability, sideband instability, or most frequently, modulational instability. The present study considers only the initial conditions in which the Stokes solution is modulated by the most unstable wave number $q=q_{\max}=1$ as follows:

$$\psi(x,0)=1+0.1e^{i\theta}\cos(q_{\max}x), \tag{4}$$

where $0.1e^{i\theta}$ indicates the initial amplitude of the modulation. We investigate the long-time evolution as we vary θ from 0° to 90° by means of numerical integration. Time integration is effected by using a predicting leap-frog scheme with a correcting trapezoidal step, which is accurate to second order without a time-splitting instability.[6] A pseudospectral numerical method is employed for space integration.[7]

When $\theta=0°$, we recover the same long-time evolution as shown in Ref. 8, which is also displayed in Fig. 1(a). Here, the evolution leads to a periodic collapse (forming a localized wave packet) and broadening on a long time scale. This behavior has been referred to as the FPU (Fermi-Pasta-Ulam) recurrence phenomenon[8] for a historical reason. We have found that there are actually two types of evolutionary patterns possible as we vary θ from 0° to 90°. The other type (see also Ref. 9) is displayed in Fig. 1(b), which is obtained when θ is set to 90°. In this evolution, the localized wave packets (LWP) recur differently in that the following LWP's are displaced almost out of phase from the previous sites. By comparison, the recurrence period of Fig. 1(b) is about

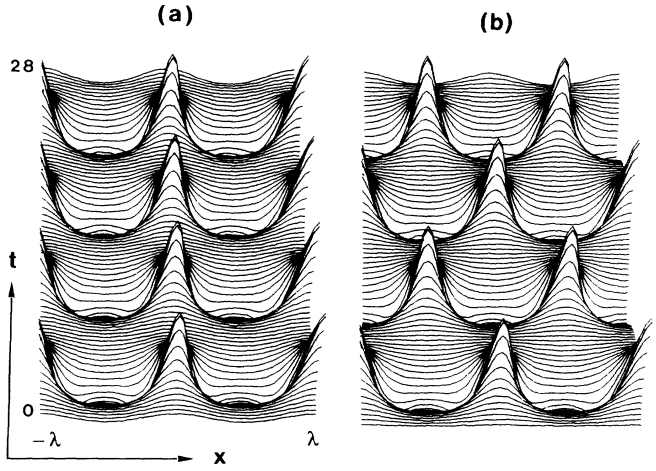

FIG. 1. Two types of evolution patterns. Envelope amplitude $|\psi|$ is plotted. (a) $\theta=0°$; (b) $\theta=90°$.

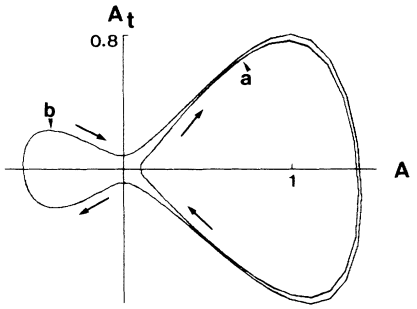

FIG. 2. Phase trajectories. The orbit denoted by a is obtained directly from the pattern of Fig. 1(a). Orbit b is taken from the flip-flop pattern of Fig. 1(b). Arrows indicate the directions of motion. It is expected that there exists an HMO passing through the origin in between a and b.

twice as long as that of Fig. 1(a). This flip-flop character starts to appear as θ is raised beyond 45°; thus, for θ less than 45°, the first pattern of Fig. 1(a) is realized while, for $45° \leq \theta \leq 90°$, the second pattern of Fig. 1(b) determines the long-time evolution.

What makes the difference between the two definite evolutionary patterns? To answer the question, we need to investigate the corresponding dynamics in the phase space formed by the following two dynamic variables. These are

$$A(t) = |\psi(0,t)| - 1 , \tag{5a}$$

$$A_t(t) = dA(t)/dt ; \tag{5b}$$

thus, $A(t)$ represents the amplitude-norm departure from equilibrium at the origin. This diagnostic measure turns out to provide crucial information. The phase trajectories taken from Fig. 1 are shown in Fig. 2. The trajectory denoted by a is obtained directly from the evolution pattern shown in Fig. 1(a), while orbit b is taken from the flip-flop pattern of Fig. 1(b). Note that orbit b possesses two (stable) paths into the origin, $(A,A_t) = (0,0)$, as well as two (unstable) paths pushed away from the origin. This implies that the origin could be a saddle point. If so, orbit b suggests that the separatrix passing through the origin in an asymmetric double-loop-type homoclinic orbit. The FPU recurrence of Fig. 1(a) is then the trapped motion within one lobe of this asymmetric HMO. A well-known property[10] of an HMO is that, as an orbit approaches an HMO, the orbit period increases and in the immediate vicinity of an HMO, the orbit period diverges. We observe this property near the transition angle $\theta = 45°$, which is to be seen in Figs. 3 and 4. Figure 3(a) exhibits the evolution for $\theta = 44.9°$ and Fig. 3(b) displays the pattern for $\theta = 45°$ for the same time interval as in Fig. 1. As shown in Fig. 3, both patterns exhibit much larger recurrence periods. The corresponding phase motions are shown in Fig. 4. For simplicity, we only present the orbit taken from the

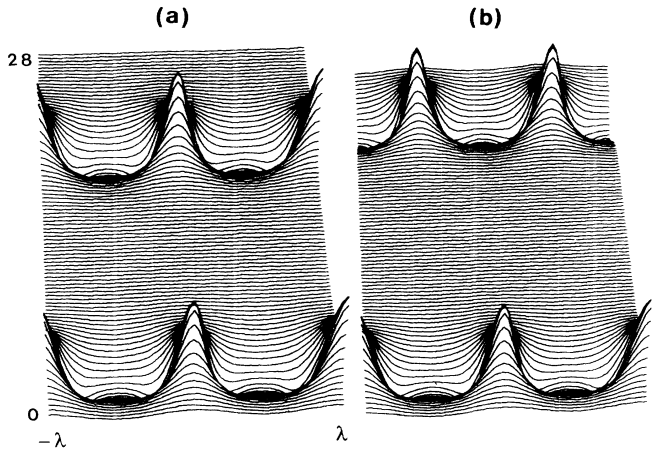

FIG. 3. Evolutions for (a) $\theta = 44.9°$ and (b) $\theta = 45°$. By comparison with the patterns in Fig. 1, the recurrence periods are seen to be much larger.

pattern of Fig. 3(b), which is denoted by b in Fig. 4. Note that the phase orbit corresponding to Fig. 1(b) is also shown for comparison. The × mark on orbit b indicates the starting point. It is observed that the trajectory has not yet completed its orbital motion as it spends much of its time near the origin. The reason that we do not see an infinite period here is because of the initial choice of amplitude in (4), which keeps the orbit a certain distance away from the HMO. As we decreased the initial amplitudes in (4), we actually observed orbits with periods that are much larger. The observations made so far lead to the conclusion that the origin is truly a saddle point.

We now turn to a discussion of the main goal of the Letter, which is concerned with the sensitivity of the behavior near the HMO as the Hamiltonian constraint is released, as well as the associated pattern dynamics in real space. For instance, one encounters the following

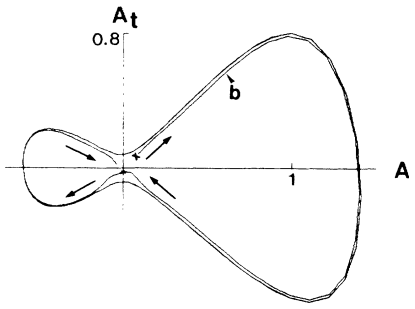

FIG. 4. Motion in phase space. The orbit denoted by b is taken from the pattern of Fig. 3(b). For comparison, the orbit corresponding to Fig. 1(b) is also shown. The × mark indicates the starting point. Note that the trajectory spends much of its time near $A = 0$ before being pushed away.

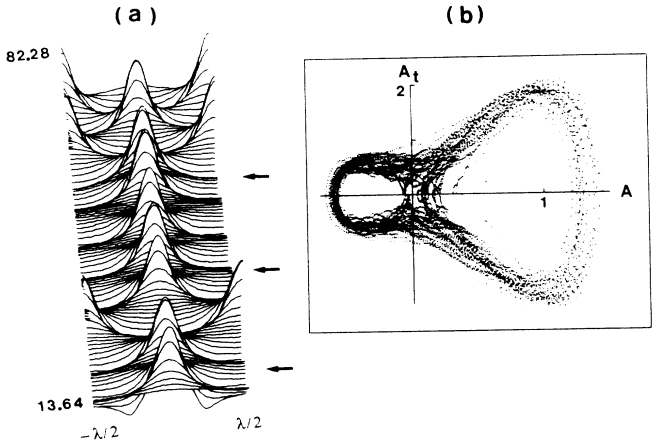

FIG. 5. Perturbed NLS. (a) The evolution exhibits a random combination of the two patterns. Arrows indicate the moments of pattern change. (b) Corresponding motions in the phase space for $0 \leq t \leq 440$. Notice the irregular HMO crossings.

perturbed NLS in plasma physics when a uniform plasma is driven by an external rf field:[11]

$$i\psi_t + \psi_{xx} + |\psi|^2\psi = -i(\sigma\psi + ge^{i\pi t}) . \quad (6)$$

Here, we consider the initial condition which has led to orbit b in Fig. 4, i.e., $\theta = 45°$ in Eq. (4). Chaos is found for $\sigma = 0.0001$ and $g = 0.0035$. The chaotic motions are displayed in Fig. 5. Figure 5(a) shows an evolution which exhibits a random combination of the two patterns of Figs. 1(a) and 1(b). The evolution is displayed for $13.64 \leq t \leq 82.28$ and arrows indicate the moments of pattern change. Figure 5(b) exhibits the corresponding phase motions during $0 \leq t \leq 440$, where one observes irregular HMO crossings. Figure 5 demonstrates that the irregular HMO crossings correspond to the chaotic oscillations, or selections, between the two patterns. Equivalently, Fig. 5 illustrates that the presence of an HMO is a potential source of complicated pattern dynamics. It is noted that as the evolution keeps its even parity under the given initial conditions of (4), the chaotic motions observed would probably be characterized by an attractor of the lowest dimension of the system.

In closing, we remark that the modulated Stokes solution has been proven, both experimentally[12] and numerically,[8] to comprise two frequencies; one, a shifted Stokes frequency and the other, a much slower modulational frequency. The present study then implies that this two-torus motion loses its stability to a chaotic motion through a homoclinic instability.

The author acknowledges the support of the Korean Science and Engineering Foundation through Grant No. SG-2001460. He also thanks the University Computing Center for the computer time used in this study.

[1]Ilya Prigogine and Isabelle Stengers, *Order Out of Chaos* (Bantam, New York, 1984).

[2]A. R. Bishop, D. W. McLaughlin, M. G. Forest, and E. A. Overman, II, Phys. Lett. A **127**, 335 (1988); M. G. Forest, in *Nonlinear Evolutions,* edited by Jérôme J. P. Leon (World Scientific, Singapore, 1988).

[3]H. T. Moon and M. V. Goldman, Phys. Rev. Lett. **53**, 1821 (1984); H. T. Moon, Phys. Rev. Lett. **57**, 1883 (1986).

[4]V. E. Zakharov and A. B. Shabat, Zh. Eksp. Teor. Fiz. **61**, 118 (1971) [Sov. Phys. JETP **34**, 62 (1972)].

[5]T. B. Benjamin and J. E. Feir, J. Fluid Mech. **27**, 417 (1967).

[6]Jenö Gazdag, J. Comput. Phys. **20**, 196 (1976).

[7]B. Fornberg and G. B. Whitham, Philos. Trans. Roy. Soc. London **289**, 373 (1978).

[8]H. C. Yuen and W. E. Ferguson, Phys. Fluids **21**, 1275 (1978).

[9]E. R. Tracy, H. H. Chen, and Y. C. Lee, Phys. Rev. Lett. **53**, 218 (1984).

[10]J. Guckenheimer and P. Holmes, *Nonlinear Oscillations, Dynamical Systems, and Bifurcations of Vector Fields* (Springer-Verlag, Berlin, 1983).

[11]G. J. Morales and Y. C. Lee, Phys. Rev. Lett. **33**, 1016 (1974).

[12]B. M. Lake, H. C. Yuen, H. Rungaldier, and W. E. Ferguson, J. Fluid Mech. **83**, 49 (1977).